

Vanishing Atomic Migration Barrier in SiO₂

Michael J. Aziz[†], Susan Circone* and Carl B. Agee*

[†]Division of Engineering and Applied Sciences, Harvard University, Cambridge MA 02138;
maziz@harvard.edu

*Department of Earth and Planetary Sciences, Harvard University, Cambridge MA 02138

Understanding the high-pressure behaviour of SiO₂, a prototypical network-forming material, is important for resolving many problems in the Earth sciences. For pressures up to 1-3 GPa ($1-3 \times 10^4$ atm), it has been shown that increases in pressure result in higher rate constants for atomic transport processes such as diffusion, viscous flow and crystal growth in SiO₂ as well as in some silicate melts¹⁻⁵. Structural transitions and coordination changes observed beyond 10 GPa (refs. 5-9) may also be related to this pressure-induced increase in atomic mobility. There must be limits, however, on the extent to which pressure can enhance mobility, as a migration barrier decreasing linearly with pressure should vanish at a critical pressure, beyond which a sudden change in behaviour should be observed^{10, 11}. Here we report measurements of the pressure-dependence of the growth rate of quartz from amorphous SiO₂ for pressures up to 6 GPa. We observe a sharp peak in growth rate — implying a minimum in viscosity — at 3 GPa, which we interpret as evidence that the critical pressure is being traversed. The corresponding depth below the Earth's surface at which this peak occurs (~ 100 km) suggests that this critical pressure may be related to the ubiquitous cut-off in subduction-related volcanism observed when oceanic plates reach approximately this depth.

The relationship between crystal growth rate ν and viscosity η or diffusivity D of network formers has been well established¹², especially for oxides¹³:

$$\nu = f [D / \lambda] [1 - \exp(-nG/kT)], \quad (1)$$

where f is the fraction of interfacial sites at which the growth reaction can occur, D is the diffusivity, λ is the bond length, G is the change in Gibbs free energy per molecular unit crystallized, and n is the number

of units crystallized per thermally-produced defect at the interface before defect annihilation. D can be replaced by the inverse of the viscosity, η , through the Stokes-Einstein relation $D = kT/3\eta$. Thus a measurement of ν gives us insight into the behavior of other atomic transport processes such as diffusion and flow.

Crystallization experiments were performed in a multi-anvil solid-medium apparatus¹⁴ at 1673 K and 2.5 - 8.0 GPa pressure (P). The crystal growth morphology is similar to that of Fratello et al.². Measured growth rates at 2.5 GPa coincide with those of Fratello et al. for this material and the rates obtained at 3 GPa are consistent with an extrapolation of their data obtained between 0.5-2.5 GPa (Fig. 1), following the *exponential increase of ν with P* . In marked contrast, ν *decreases with P* from 3 to 6 GPa. The pressure-dependence of the rate is characterized by the apparent activation volume, $V^* = -kT (\ln \nu / P)_T$ (solid lines in Fig. 1). The data for $P < 3$ GPa are fit by $V^* = -19.2 \pm 1.5 \text{ cm}^3/\text{mol}$; the 3 - 6 GPa data are fit by $V^* = +5.2 \pm 1.6 \text{ cm}^3/\text{mol}$.

The change in behavior at 3 GPa might be due to either of the bracketed factors in eq. (1). Fratello et al. assumed that over the limited pressure range sampled by their experiment the thermodynamic factor $[1 - \exp(-nG/kT)]$ is constant, thereby attributing all of the change in ν with P to the kinetic, or mobility factor $[D/\eta]$. (They used the lack of curvature in the low P data to conclude $n \gg 1$.) Because of its high compressibility, $\alpha\text{-SiO}_2$ is expected to become more stable than quartz at very high pressure¹⁵, whereupon the thermodynamic factor reduces the growth rate to zero. At 1673 K, $-G(P)$ calculated¹⁶ from literature thermodynamic data starts at zero near 0 GPa, reaches a maximum of 7 kJ/mol near 6 GPa, and crosses zero again near 16.4 GPa. Inserting $-G(P)$ into eq. (1) and assuming a constant value for $-kT (\ln [D/\eta] / P)_T$ yields the dashed curve in Fig. 1. Under no combination of thermodynamic uncertainties can the measured behavior be explained by variations in the final bracketed factor in eq. (1); rather than decreasing, this thermodynamic factor increases slightly over the range 3-6 GPa, whereas at 6 GPa ν itself falls below the dashed curve by approximately two orders of magnitude. Hence we must attribute the effect to the mobility factor, $[D/\eta]$.

A vanishing migration barrier might occur in several ways. In Fig. 2 we show how it could occur for a mechanism in which crystal growth is caused by the migration of defects at the interface, during which the defect configuration alternates between two states with differing densities. Fig. 2a indicates how the standard Gibbs free energy might vary during defect formation and migration. If state C is denser

than B then the pressure-dependence of these potentials for a pair of adjacent states B and C will be as shown in Fig. 2b. At P_c the migration barrier ($G_m = G_C^o - G_B^o$) vanishes although the barrier to defect formation ($G_f = G_B^o - G_A^o$) remains nonzero. For $P > P_c$, pressure has so destabilized B that C becomes more stable and a high-P barrier to migration appears as $G_m^{hiP} = G_B^o - G_C^o$. At all P the mobility factor in eq. (1) is proportional to $\exp -\frac{1}{kT} \times (\max\{G_C^o, G_B^o\} - G_A^o)$, displaying a sharp peak at P_c . This interpretation leads to the interesting prediction of a soft vibrational mode about state B near P_c , perhaps observable with neutron diffraction.

There is growing evidence that network structures tend to have negative activation volumes for atomic transport processes^{1-5, 17}. Generally for defect-mediated processes $V^* = V_f + V_m$, with the formation volume $V_f = G_f / P$ and the migration volume $V_m = G_m / P$. Hence at least one of V_f and V_m tends to be negative, implying a "free energy catastrophe" at a critical pressure where a barrier to either formation or migration vanishes. The associated peak in the P-dependence of atomic transport rates may be a general phenomenon for network structures. Although possibly related fundamentally, the observed phenomena leading to the proposed vanishing migration barrier can be contrasted with the shear instability proposed for amorphization^{7, 18}. Our observation that quartz and a-SiO₂ continue to exist well past P_c shows that a migration barrier can vanish well before the onset of any shear instability.

This interpretation provides reasonable values of the relevant parameters. The apparent activation volume (with thermodynamic factor constant) for $P < P_c$ is $V^* = V_C - V_A = V_f + V_m$ and for $P > P_c$ is $V^{*,hiP} = V_B - V_A = -V_f$, where we define $V_m = V_C - V_B$ and $V_f = V_B - V_A$ such that they are always reckoned from the low-P side of P_c . Using the data in Fig. 1, this interpretation yields $V_m = -24.4$ cm³/mol and $V_f = +5.2$ cm³/mol. Given a vanishing migration barrier at P_c , we can deduce approximate energies of migration and formation using $G = E + pV - TS$. With no reliable estimates of the entropies of formation and migration, initially we arbitrarily set them to zero (an assumption to be revisited below), resulting in $E_m - P_c V_m = 73$ kJ/mol, $E_f = E^* - E_m = 195$ kJ/mol, where we have used Fratello's value of $E^* = 268$ kJ/mol.

Fratello et al. demonstrated that the presence of trace amounts of OH or Cl are very important in determining the growth rate over the entire range studied (< 10 to 20,000 molar ppm). Similar behavior has been demonstrated for diffusion in silicates⁴. Everybody's experimental results are likely to have

been obtained in the presence of impurity concentrations in this range, as even nominally "anhydrous" minerals have plenty of OH¹⁹. Therefore laboratory experimental results may be compared directly to natural processes such as those occurring in the earth's interior. Molecular dynamics simulations of truly anhydrous material, showing a broad maximum in the diffusivity with increasing pressure^{20, 21}, may be focusing on a hydrogen-free process that occurs only at much higher temperatures.

A specific example of a mechanism consistent with all of the above observations is the Spaepen-Fratello model^{22, 23}, which has been used to account successfully for quartz growth rates below 3 GPa and for the observed solid phase epitaxial crystallization behavior of pure amorphous Si¹¹. The mechanism involves the thermal rupture of Si-O bonds at Si-O-Si-OH, leading to a sequence of migration events, alternating between O undercoordination (state "B") and Si overcoordination (state "C"). Their proposed mechanism is shown in Fig. 2c; they also showed how multiple migration steps can reconstruct the amorphous network into the crystalline structure before defect annihilation. OH not only can catalyze the rupture but can also give more mobility to the resulting non-bridging O-Si-OH by reducing network constraints. The structural nature of the negative migration volume in this model is evident.

The negative migration volume is very likely due a transition state (TS) ("C" in Fig. 2) involving high-coordination Si, but its exact nature is still a matter of debate. It may be due to an overcoordination state that is sixfold (octahedral) Si^{21, 24}. Our inferred migration energy and volume are close to the P=0 molar energy and volume differences between the high-pressure stishovite phase (edge-sharing SiO₆ octahedra) and a-SiO₂ (corner-sharing SiO₄ tetrahedra): they are 1.6 and 1.8 times these molar energy and volume differences. So a TS composed of 1-2 SiO₂ units with an energy and volume similar to that of stishovite is quite reasonable. Alternatively, the overcoordination state may be fivefold^{20, 22, 23, 25}, as illustrated in Fig. 2c, because a five-fold coordinated Si state might not be significantly different in energy and volume. Both high-coordination states have been detected in silicate glasses quenched from 6 GPa and above²⁵. However, a coesite-like saddle-point structure (four-membered rings of corner-sharing SiO₄ tetrahedra) is very unlikely, as the energy and volume differences with the amorphous phase are too low: to match the inferred migration energy, the TS configuration would have to be composed of ~ 10 SiO₂ units in the coesite structure. Poe et al.¹⁷ recently reported a peak in O diffusivity in Na₃AlSi₇O₁₇ at 8 GPa and attributed it to a measured²⁵ peak in the concentration of 5-coordinated Al. Our measured peak in pure SiO₂ indicates that transitory Si coordination changes cannot be ignored as low as 3 GPa.

In absolute magnitude, the measured growth rate at P_c is consistent with the rate expected from athermal migration of non-bridging oxygen. The thermodynamic factor in eq. (1) is about 0.34 near P_c . The site factor f is $C_i \exp(-G_f/kT)$ where C_i is the mole fraction of catalyzing impurity (OH and Cl) at the interface. Assuming no preferential adsorption of impurity at the interface we set C_i to its value in the bulk, $\sim 4 \times 10^{-4}$. From our interpretation of the data, the defect formation enthalpy is $H_f = E_f + P_c V_f = 210$ kJ/mol, resulting in the fraction of Si-O-Si-OH sites that have ruptured at P_c being $\exp(-G_f/kT) = 2.7 \times 10^{-7}$ (assuming the unknown formation entropy is zero), yielding $f = 1.1 \times 10^{-10}$. With a vanishing migration barrier, $[D/]$ should attain its maximum value, the velocity of athermal migration; this should be near the speed of sound or $\sqrt{kT/m}$; both are roughly 1 km/sec. Eq. (1) then gives a peak growth rate of roughly 100 nm/sec, to be compared with the experimental value of 1000 nm/sec. Preferential impurity segregation to the interface and a positive defect formation entropy could easily account for the difference. The latter, in cases where it has been determined (metals and Si), provides multiplicative factors of $10^{1\pm 1}$.

It is perhaps no coincidence that the enthalpy difference between stishovite and α -SiO₂ vanishes near our measured P_c : at 4.7 GPa at our experimental temperature of 1673 K. Additionally, the pressure at which extrapolations indicate that it vanishes at 4000 K, 3.9 GPa, is within the range of pressures for the maximum in oxygen diffusivity vs. P in the molecular-dynamics simulations of Tsuneyuki and Matsui²¹. They suggested that the relevant enthalpy difference is between stishovite and coesite, but this difference does not vanish under the conditions of our experiment until 8.4 GPa - three times as far away from the measured P_c .

Why should the difference in H , rather than the difference in G , between the reactant well and the TS vanish near P_c ? According to Transition State Theory (TST) the activation barrier is in G rather than H . However, in TST the TS is constrained to have one less vibrational degree of freedom than the bulk phases, which implies that although E, V , and H might be nearly the same as for bulk phases, the entropy necessarily differs from that of a bulk phase. Furthermore, in classical canonical TST²⁶ there is a Maxwell-Boltzmann distribution of positions and velocities throughout the reactant well ("B" in Fig. 2a). An increased (decreased) entropy of the TS region ("C") of configuration space increases (decreases) the reaction rate. However, as P_c is approached from below and the barrier becomes small enough, escape occurs from the reactant well with incomplete thermalization, reducing the importance of the entropy of the TS region of configuration space. Hence in the small-barrier limit, the barrier to a reaction might more

appropriately be in H rather than in G. This limit is reminiscent of collision theory²⁷. High pressure may thus represent an opportunity for condensed-matter chemical kineticists to investigate systematically the behavior of kinetic rate constants when kinetic barriers vanish under controllable conditions.

The enhancement of transport rate in the range 0-3 GPa is very large, implying a significant inverse effect on viscosity of certain rocks and magmas with depth. This is consistent with the experimental work of Kushiro on network structured melts. Our results may be highly relevant to subduction zone magmatism in the mantle. In this setting partial melting produces magmas enriched in SiO₂. Although there is little experimental information on the competing effect of temperature on silica-rich melts at high pressure, we propose that such magmas may show a decrease in viscosity with depth until the migration barrier vanishes at 3 GPa (a depth of ~ 100 km), and then suddenly start to become more viscous. We expect that this increase in viscosity may impede silicic magma mobility deeper than 100 km. Interestingly, the predicted viscosity minimum coincides with the nearly constant depth to the Wadati-Benioff zone locating the subduction slab at ~100 km beneath most subduction related volcanic fronts²⁸. This constant depth appears to be largely unaffected by such factors as convergence rate or slab thermal structure. We speculate that the onset of an increasing magma viscosity at a "universal" depth of 100 km, predicted from the present experimental results, may control this aspect of subduction zone dynamics. There are many unanswered questions such as the effect of SiO₂ content and volatiles on the pressure of the viscosity minimum. The proposed magma viscosity minimum at 3 GPa is a testable hypothesis. Unfortunately, all existing high pressure experimental data on magma viscosity are limited to 2.5 GPa. Viscosity measurements in the range 2.5 to 5 GPa should be considered a high priority.

References

1. Kushiro, I. in *Physics of Magmatic Processes* (ed. Hargraves, R.B.) 93-120 (Princeton University Press, Princeton, NJ, 1980).
2. Fratello, V.J., Hays, J.F. & Turnbull, D., "Dependence of growth rate of quartz in fused silica on pressure and impurity content", *J. Appl. Phys.* **51**, 4718-28 (1980).
3. Shimizu, N. & Kushiro, I., "Diffusivity of oxygen in jadeite and diopside melts at high pressures", *Geochim. Cosmochim. Acta* **48**, 1295-1303 (1984).
4. Goldsmith, J.R., "Enhanced Al/Si Diffusion in KAlSi₃O₈ at High Pressures: The Effect of

- Hydrogen", *J. Geol.* **96**, 109-124 (1988).
5. Stebbins, J.F., McMillan, P.F. & Dingwell, D.B., eds., *Structure, Dynamics and Properties of Silicate Melts*, Reviews in Mineralogy vol. **32** (Mineralogical Society of America, Washington, 1995).
 6. Williams, Q. & Jeanloz, R.P., "Spectroscopic Evidence for Pressure-Induced Coordination Changes in Silicate Glasses and melts", *Science* **239**, 902-905 (1988).
 7. Hemley, R.J., Jephcoat, A.P., Mao, H.K., Ming, L.C. & Manghnani, M.H., "Pressure-Induced Amorphization of Crystalline Silica", *Nature* **334**, 52-54 (1988).
 8. Tsuchida, Y. & Yagi, T., "New Pressure-Induced Transformations of Silica at Room Temperature", *Nature* **347**, 267-269 (1990).
 9. Meade, C., Hemley, R.J. & Mao, H.K., "High Pressure X-ray Diffraction of SiO₂ Glass", *Phys. Rev. Lett.* **69**, 1387-1390 (1992).
 10. Nygren, E., Aziz, M.J., Turnbull, D., Poate, J.M., Jacobson, D.C., Hull, R., "Pressure Dependence of Arsenic Diffusivity in Silicon", *Appl. Phys. Lett.* **47**, 105-107 (1985).
 11. Lu, G.-Q., Nygren, E. & Aziz, M.J., "Pressure-Enhanced Crystallization Kinetics of Amorphous Si and Ge: Implications for Point Defect Mechanisms", *J. Appl. Phys.* **70**, 5323-5345 (1991).
 12. Spaepen, F. & Turnbull, D., "Crystallization Processes", in *Laser Annealing of Semiconductors* (eds. Poate, J.M. & Mayer, J.W.) 15-42 (Academic, New York, 1982).
 13. Jackson, K.A., Uhlmann, D.R. & Hunt, J.D., "On the nature of crystal growth from the melt", *J. Crystal Growth* **1**, 1-36 (1967).
 14. Walker, D., Carpenter, M.A. & Hitch, C.M., "Some Simplifications to Multi-Anvil Devices for High Pressure Experiments", *Amer. Mineral.* **75**, 1020-1028 (1990).
 15. Hemley, R.J., Mao, H.K., Bell, P.M. & Mysen, B.O., "Raman Spectroscopy of SiO₂ Glass at High Pressure", *Phys. Rev. Lett.* **57**, 747-50 (1986).
 16. Circone, S., Aziz, M.J. & Agee, C.B., (unpublished).
 17. Poe, B.T., McMillan, P.F., Rubie, D.C., Chakraborty, S., Yarger, J., Diefenbacher, J., "Silicon and Oxygen Self-Diffusivities in Silicate Liquids Measured to 15 Gigapascals and 2800 Kelvin", *Science* **276**, 1245-8 (1997).
 18. Tse, J.S. & Klug, D.D., "Mechanical Instability of α -Quartz: A Molecular-Dynamics Study", *Phys.*

Rev. Lett. **67**, 3559-3562 (1991).

19. Meade, C., Reffner, J.A. & Ito, E., "Synchrotron infrared absorbance measurements of hydrogen in MgSiO₃ perovskite", *Science* **264**, 1558-60 (1994).
20. Angell, C.A., Cheeseman, P.A. & Tamaddon, S., "Pressure Enhancement of Ion Mobilities in Liquid Silicates from Computer Simulation Studies to 800 Kilobars", *Science* **218**, 885-887 (1982).
21. Tsuneyuki, S. & Matsui, Y., "Molecular dynamics study of pressure enhancement of ion mobilities in liquid silica", *Phys. Rev. Lett.* **74**, 3197-3200 (1995).
22. Spaepen, F. & Turnbull, D., "Kinetics of motion of crystal-melt interfaces", *AIP Conf. Proc.* **50**, 73-83 (1979).
23. Fratello, V.J., Hays, J.F., Spaepen, F. & Turnbull, D., "The mechanism of growth of quartz crystals into fused silica", *J. Appl. Phys.* **51**, 6160-4 (1980).
24. Stolper, E.M. & Ahrens, T.J., "On the Nature of Pressure-Induced Coordination Changes in Silicate Melts and Glasses", *Geophys. Res. Lett.* **14**, 1231-1233 (1987).
25. Stebbins, J.F., "Dynamics and Structure of Silicate and Oxide Melts: Nuclear Magnetic Resonance Studies", in *Structure, Dynamics and Properties of Silicate Melts* (eds. Stebbins, J.F., McMillan, P.F. & Dingwell, D.B.) 191-246 (Mineralogical Society of America, Washington, 1995).
26. Vineyard, G.H., "Frequency Factors and Isotope Effects in Solid State Rate Processes", *J. Phys. Chem. Solids* **3**, 121-127 (1957).
27. Laidler, K.J. *Chemical Kinetics* (Harper & Row, 1987).
28. Gill, J. *Orogenic Andesites and Plate Tectonics* (Springer-Verlag, Berlin, 1981).
29. Agee, C.B., Li, J., Shannon, M.C. & Circone, S., "Pressure-Temperature Phase Diagram for the Allende Meteorite", *J. Geophys. Res.* **100**, 17725-17740 (1995).

Acknowledgements. This research was supported by the Harvard MRSEC under NSF-DMR-94-00396. We thank R.P. Jeanloz for helpful discussions.

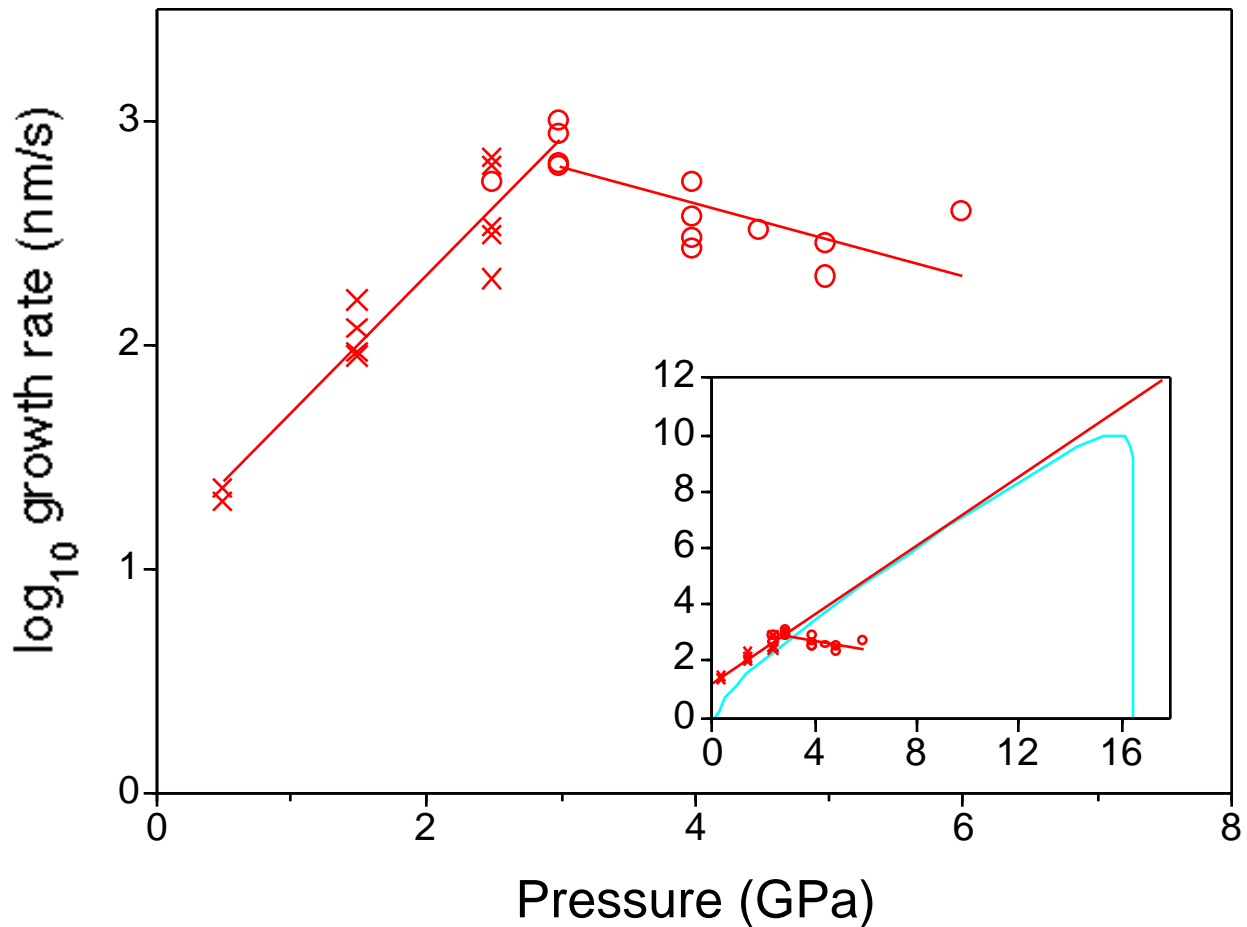


Fig. 1. Quartz growth rate at 1673 K vs. pressure. Growth rates were measured on Spectrosil W.F., an amorphous silica ($a\text{-SiO}_2$) containing 2.360 molar ppm Cl and 30 ppm OH. The experimental setup²⁹ and sample preparation procedure² are described elsewhere. Specimens were pressurized at room temperature, heated gradually to 1073 K and rapidly from 1073 to 1673 K, held at constant T for several minutes, quenched rapidly to < 473 K, then slowly decompressed at room temperature. Axial sectioning determined the extent of crystal growth. Although coesite is the stable phase above 3 GPa, quartz nucleated on the Pt capsule up to 5 GPa. Above 5 GPa coesite nucleates unless the sample surface is "seeded" with finely-ground natural quartz. The growth rate is unaffected by the presence of quartz seeds: the measured quartz growth rate from a 4 GPa seeded experiment coincides with those from unseeded experiments. At 8 GPa copious coesite nucleation precludes the measurement of a quartz growth rate. Measured growth rates indicated by crosses² and circles (this study). Apparent activation volumes with opposite signs are obtained from the slope of the straight lines fit to the data below and above 3.0 GPa. Inset: same straight-line fit to low-P data is shown to higher P along with dashed curve from eq. (1): ν plunges to zero near 0.086 and 16.4 GPa, where $G = 0$.

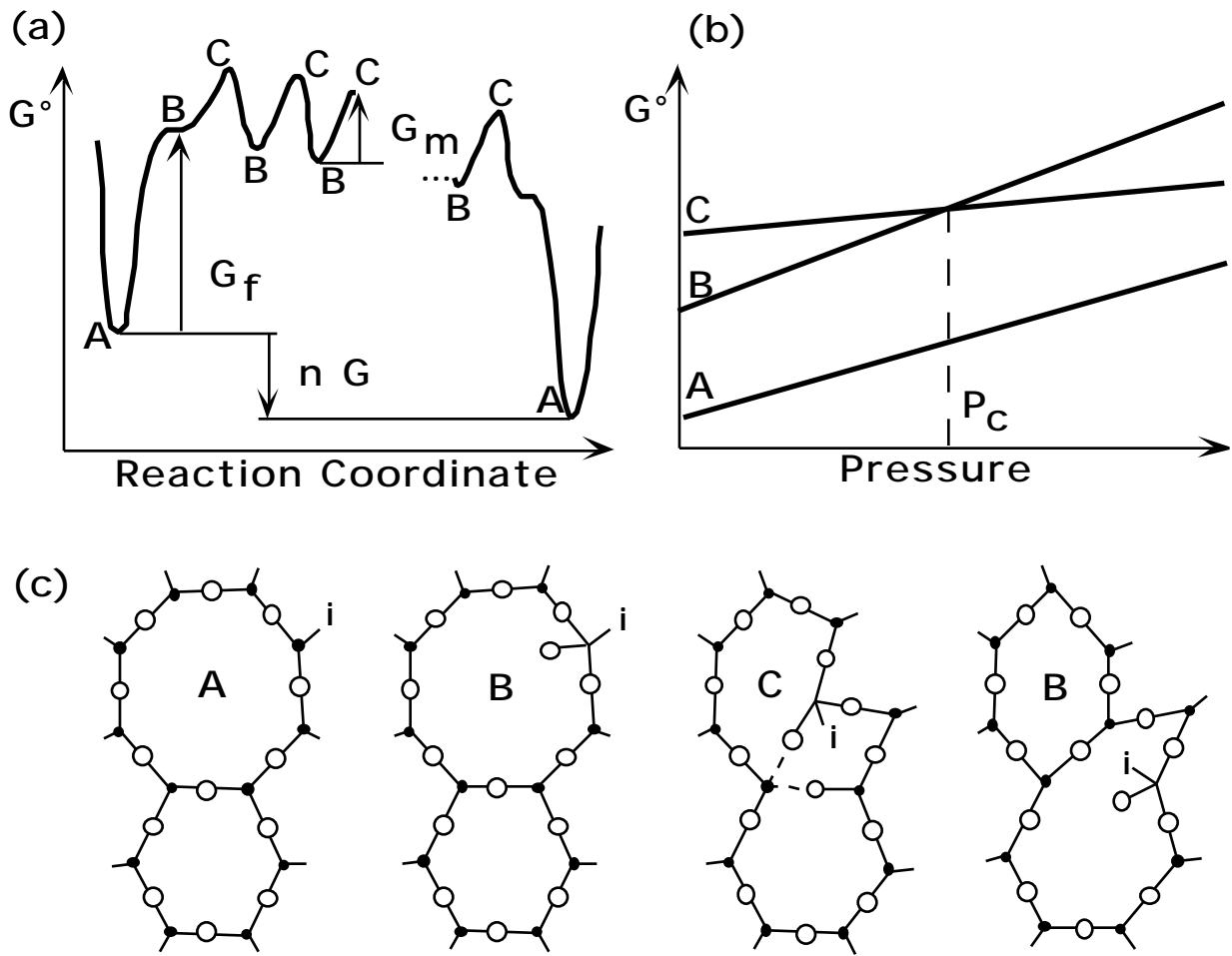


Fig. 2: Pressure-induced vanishing of atomic migration barrier due to "free energy catastrophe". (a) Standard Gibbs free energy vs. configuration for 3 states: A: quartz + a-SiO₂ + interface with no defect; B: same system with defect in high-volume state; C: same system with defect in low-volume state. The "reaction coordinate" is a path through configuration space along which the reaction proceeds; it is proportional to the number of atoms in the crystal. (b) Pressure dependence: by the thermodynamic relation $(G/P)_T = V$, the slopes of curves A, B, and C are the volumes, V_A , V_B , and V_C , of the system in these respective configurations. (c) Possible migration mechanism, adapted from Fratello et al.²³ (see also Fig. 17 of Stebbins²⁵), alternating between low-coordination state B (non-bridging O) and high-coordination state C (overcoordinated Si). Si is at each vertex; solid circles represent Si-O bonds normal to the page. "i" is catalyzing impurity (OH or Cl). It is reasonable to suppose that the barrier to migration doesn't entirely vanish because G° values between points B and C in (a) do not necessarily remain bounded by the values at B and C as P_c is approached. Additionally, near P_c some topography may develop in orthogonal directions revealing new local minima.